Energy Proceedings
Vol 52, 2025
ISSN 2004-2965

Catalyst Layer Design for High Reversal and Free Radical Tolerance Membrane Electrode Assemblies#

Yan Xiao[1], Xiangyang Zhou[2], Bing .Li[1]*, Pingwen Ming[1], Cunman Zhang[1]

1 School of Automotive Studies & Clean Energy Automotive Engineering Center, Tongji University, Shanghai, 201804, China

2 Shanghai AI NEV Innovative Platform Co., Ltd, Shanghai, 201804, China
(Corresponding author: Bing Li; Email: libing210@tongji.edu.cn)

ABSTRACT

Reactive oxygen species (ROS) produced during electrochemical reactions in proton exchange membrane fuel cells (PEMFCs), combined with the occurrence of cell reversal events, can lead to the degradation of both the catalytic layer and the proton exchange membrane. These dual challenges, which can happen simultaneously, pose significant risks to the longevity of fuel cells. In this paper, we explore the impact of incorporating $Ce_xZr_{1-x}O_2$ in the cathode and $IrRuO_2$ in the anode on the electrical performance and open-circuit durability of the membrane electrode assembly. Our findings indicate that the modified membrane electrode demonstrates exceptional open-circuit durability and resistance to voltage reversal. During a 500 h open-circuit voltage (OCV) test, nearly all voltage degradation was found to be reversible. Additionally, the hydrogen infiltration current density remained low, measuring only 5-8 mA/cm², and showed minimal variation when the inlet pressures at both the anode and cathode were increased. Moreover, the enhanced membrane electrode exhibited remarkable resistance to reverse current events. The cell reversal survival time reached 742 minutes at a current density of 200 mA/cm², with only a slight reduction in voltage and maximum power density—24 mV and 23.2 mW/cm² after the first reversal test. These results provide valuable insights for developing highly durable membrane electrodes, paving the way for advancements in fuel cell technology.

Keywords: proton exchange membrane fuel cells, catalyst layers, radical quencher, $Ce_xZr_{1-x}O_2$, durability

1. INTRODUCTION

Proton exchange membrane fuel cells (PEMFCs) are highly efficient and low-emission energy conversion devices with a wide range of applications, from portable electronics to transportation[1-3]. Despite their potential, the long-term stability and durability of PEMFCs, particularly in the catalyst layer, pose significant challenges that hinder their broader commercialization[4, 5]. The durability of a PEMFC is largely influenced by its operating conditions, including start-stop cycles and load variations, as well as the supply of reactants. Sudden changes in these conditions can lead to reactant shortages at the counter electrode. Insufficient fuel supply may increase the anode potential, cause corrosion of the carbon support, and result in cell reversal, all of which can compromise the catalyst layer's structural integrity and reduce the service life of the cell. Operational conditions like start-stop and idle phases can generate reactive oxygen species (ROS), such as peroxyl and hydroxyl radicals. These radicals can degrade the proton exchange membrane (PEM), leading to pinhole formation and facilitating hydrogen and oxygen permeation that accelerates the deterioration of the catalytic components. Furthermore, side reactions during normal operation can produce hydrogen peroxide, which decomposes into reactive radicals, further diminishing the durability of the cell[6, 7].

In response to these challenges, researchers have developed various strategies to reduce the adverse effects of ROS and voltage reversal on PEMFC components[8, 9]. One promising approach involves using cerium oxide particles, which are stable in acidic environments and can quickly recover Ce^{3+}[10, 11]. This cerium ion can be exchanged with protons in ionic membranes or incorporated into PEMs and catalyst layers[12, 13]. Kinetic modeling indicates that adding 1 wt.% Ce^{3+} significantly reduces hydroxyl radical production during fuel cell operation[14]. This finding has been supported by techniques like electron spin resonance and accelerated durability testing. In accelerated chemical stability tests, introducing 0.06 wt.% Ce into a PEM resulted in a 20-fold reduction in voltage drop rates and a three-order of magnitude decrease in the formation of harmful species compared to cells without cerium[12, 15]. However, excessive cerium content beyond this threshold negatively impacts initial

This is a paper for the 16th International Conference on Applied Energy (ICAE2024), Sep. 1-5, 2024, Niigata, Japan.

cell performance. To address issues related to reversal, researchers have introduced oxygen evolution reaction (OER) catalysts to the anode side of PEMFCs. These catalysts help maintain the water electrolysis phase during hydrogen deprivation, preventing the anode potential from exceeding 1.8 V, which reduces the risk of carbon corrosion and protects the anode from damage. Studies have shown that various OER catalysts, such as IrO_2, RuO_2, and others, can significantly enhance cell durability[3, 16-21]. For instance, Pratiti et al. demonstrated that increasing the addition of IrO_2 from 0 to 50 wt.% (relative to the anode platinum loading) extended the reversal time from 2 minutes to over 54 minutes, showcasing a substantial improvement in cell durability[17].

In conclusion, tackling the durability of PEMFCs requires a multifaceted approach. Enhancing both reversal tolerance performance and the chemical stability of the PEM simultaneously appears to be a viable strategy. However, the introduction of reversal tolerance catalysts and free radical quenchers must be carefully balanced, as they can also impact overall fuel cell performance. This study systematically investigates the synergistic effects of these components within membrane electrodes, thoroughly evaluating their influence on both the initial performance and durability of the PEMFC.

2. MATERIALS AND METHODS

2.1 Catalyst preparation and MEA assembly

In this research, we explored cerium-zirconium solid solutions ($Ce_{0.8}Zr_{0.2}O_2$, CZO) as catalysts for free radical removal, prepared using a wet technique as detailed in prior studies. The CZO catalyst was applied to the cathode side of a PEM (Gore M820.15). For the anode, $IrRuO_2$ was selected as the anti-reversal catalyst, mixed with Nafion, and then sprayed onto the anodic catalytic layer. The optimized membrane electrode assembly (MEA-D) was constructed through a precise procedure. Initially, 10 mL of high-purity water was placed in a beaker, and a specific quantity of catalyst (Pt/C, RTA, or CZO) was added. After thorough stirring, a 5% Nafion® solution was introduced, maintaining a mass ratio of Nafion® to carbon carrier of 1:3. Additionally, high-purity water and isopropanol were combined in a 1:1 volume ratio. The CZO catalyst represented 10 wt.% of the Pt/C content on the cathode, while the RTA catalyst accounted for 20 wt.% of the Pt/C content on the anode. To achieve a uniform catalyst slurry, the mixture was first subjected to ultrasound dispersion for 10 minutes, followed by high-speed shearing for 30 minutes, resulting in an ink-like consistency. This slurry was then uniformly sprayed onto both sides of a 25 cm² Nafion® membrane using specialized equipment. Following this, two gas diffusion layers (GDLs), each measuring 5.5 x 5.5 cm², were applied to either side of the catalyst-coated membrane and securely sealed with high-temperature-resistant adhesive tape. The structure of the resulting MEA-D is schematically represented in Fig. 1.

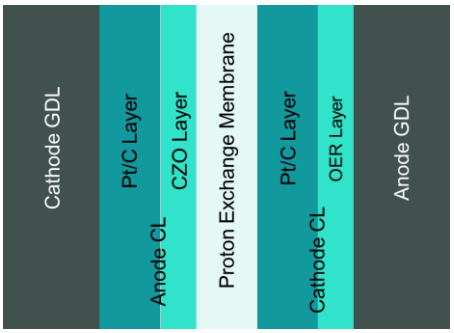

Fig. 1 Schematic structure of the MEA-D

2.2 Characterization and cell testing

To examine the morphological structure of the catalytic layer, scanning electron microscopy (SEM) was employed. The performance of the membrane electrode assembly (MEA) was assessed using the Greenlight G20 platform. In this evaluation, the stoichiometric ratios for the anode and cathode were set at 1.7:3, with the inlet gas backpressure maintained at 130 kPa for the anode and 120 kPa for the cathode. Both the inlet air and relative humidity were adjusted to 80%, and the cell temperature was consistently kept at 80 °C to ensure optimal testing conditions. For electrochemical impedance spectroscopy (EIS), a perturbation current was applied at 5% of the test current, with the frequency range spanning from 0.1 Hz to 1,000 kHz. Additionally, cyclic voltammetry (CV) tests were conducted at a scanning rate of 50 mV/s, while linear scanning voltammetry (LSV) tests were performed at 5 mV/s across a voltage range of 0.05 to 0.7 V. Throughout these tests, the inlet gas backpressure remained consistent at 130 kPa for the anode and 120 kPa for the cathode, ensuring reliable data collection. This comprehensive evaluation allows for a deeper understanding of the catalytic layer's morphology and overall MEA performance, contributing to the optimization and development of enhanced membrane electrode assemblies for fuel cell applications.

3. RESULTS AND DISCUSSION

3.1 Cell open-circuit endurance test

Fig. 2 presents a comparison of the power generation capabilities between the fabricated MEA-D and the commercially available MEA-F, which utilizes a Pt/C catalyst. The single-cell polarization and power-density curves displayed in Fig. 2a reveal that both MEA-D and MEA-F demonstrate similar performance in the low-current-density region (below 1000 mA cm^{-2}). However, as the current density increases, a noticeable divergence in performance emerges, peaking at a current density of 2000 mA cm^{-2}, where MEA-D shows a voltage drop of 180 mV compared to MEA-F. Further analysis in Fig. 2b indicates that at a current density of 1000 mA cm^{-2}, MEA-D exhibits a voltage of 0.676 V, which is 21 mV lower than that of MEA-F. Additionally, MEA-D achieves a maximum power density of 820 mW cm^{-2}, falling short by 121.4 mW cm^{-2} compared to MEA-F. The limiting current density for MEA-D is 2000 mA cm^{-2}, which is 400 mA cm^{-2} lower than that of MEA-F. These findings highlight the performance characteristics of MEA-D in comparison to MEA-F, emphasizing the strengths and limitations of the newly designed MEA under varying operational conditions.

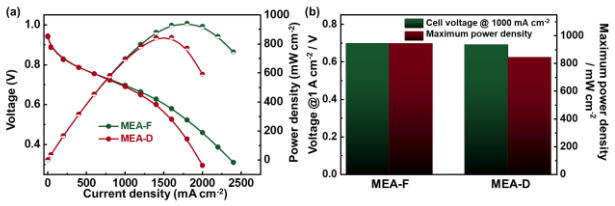

Fig. 2 (a) Initial power generation performance and (b) voltage and maximum power density at 1000 mA cm^{-2} current density for MEA-F and MEA-D

To evaluate the open-circuit durability of the MEAs, the initial performance of a single cell was assessed before transferring it to the open-circuit durability test. This test was conducted under the following conditions: cell temperature at 90 °C, relative humidity at 30%, cathode and anode inlet pressures set to 150 kPa, and hydrogen/air flow rates of 0.35/0.83 mL min^{-1}. LSV data were collected every 24 h. The test concluded when the open-circuit voltage dropped by more than 20%, the hydrogen permeation current density exceeded 15 mA cm^{-2}, or the total duration reached 500 h. Fig. 3 illustrates the cell voltage and hydrogen permeation current density over time during the open-circuit endurance test. In Fig. 3a, the open-circuit voltage of the comparison sample shows a significant decline, dropping to only 0.75 V after 50 h, with a degradation rate stabilizing at 2.78 mV h^{-1}. At this point, the hydrogen permeation current was observed at 30 μA cm^{-2}, increasing to 65 μA cm^{-2} when the pressure was lowered to 50 kPa, indicating potential perforation of the PEM. In contrast, Fig. 3c demonstrates that the voltage degradation of MEA-D is nearly reversible, maintaining an open-circuit voltage of 0.945 V even after 500 h of testing. Additionally, Fig. 3d reveals that the hydrogen permeation current density fluctuated between 5 to 8 mA cm^{-2} throughout the test, exhibiting limited correlation with variations in inlet pressures at the anode and cathode. These results suggest that MEA-D effectively mitigates damage to the PEM caused by peroxyl radicals during open-circuit conditions. Consequently, this design enhances the durability of the single cell, leading to minimal degradation of the open-circuit voltage and negligible increases in hydrogen permeation current density after 500 h of testing.

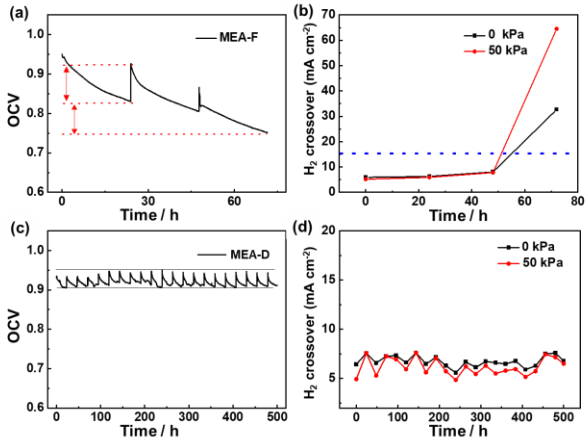

Fig. 3 Voltage and hydrogen permeation current density versus time curves for MEA-F (a) and (b), MEA-D (c) and (d) in OCV test

Following the open-circuit voltage (OCV) test, the MEA was stored overnight. The next day, after preactivation, it underwent various evaluations, including single-cell power generation tests, EIS at current densities of 400 and 1000 mA cm^{-2}, and in-situ cyclic voltammetry of the cathode. The comparative results of these tests, both before and after the OCV assessment, are presented in Fig. 4. As illustrated in Fig. 4a, while the initial performance of the comparison sample was superior, it experienced significant degradation after 70 h of the open-circuit endurance test. Specifically, the initial voltage declined by over 100 mV, and the maximum power output dropped by more than 50%, reaching only 450 mW cm^{-2}, with a decay rate of 7.14 mW cm^{-2} h^{-1}. In contrast, the MEA-D sample showed more resilience; its open-circuit voltage decreased by merely 20 mV after

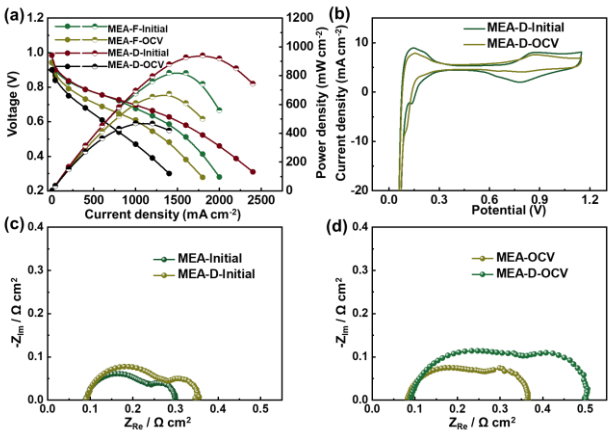

Fig. 4 Membrane electrode open-circuit endurance test before and after (a) power generation performance, (b) cathode in-situ CV curves, and EIS curves for (c) initial and (d) after open-circuit endurance at 400 mA cm^{-2}

the OCV test. Although the maximum power did decline significantly, the durability after 500 h was impressive, exhibiting a decay rate of only 0.3 mW cm^{-2} h^{-1}, reflecting a reduction of 95.8%. This demonstrates that the inclusion of a free radical quencher markedly enhances the open-circuit durability of the cell. Fig. 4b presents the in-situ cyclic voltammetry curves for the cathode, revealing a notable decline in the electrochemical active surface area (ECSA) of the MEA-D-OCV. This reduction is primarily attributed to prolonged cathode potentials exceeding 0.9 V, which can cause detrimental effects such as corrosion of the carbon supports in the catalyst layer, as well as the dissolution and agglomeration of platinum particles, ultimately leading to decreased catalyst ECSA. These adverse impacts can further compromise the power generation performance of the cell. Fig.s 4c and 4d depict the AC impedance plots of both membrane electrodes at a current density of 400 mA cm^{-2} after the endurance test. The data indicate a significant increase in both activation and mass transfer polarization for the MEA post-OCV test. The rise in activation polarization is primarily due to the degradation of dissociated aggregates, which affects the three-phase interface. Meanwhile, the increase in mass transfer polarization can be attributed to the corrosion of the carbon support material in the catalytic layer. In contrast, the MEA-D-OCV demonstrated relatively constant ohmic impedance, along with only minor increases in cathodic activation and mass transfer polarization, highlighting its improved stability under the tested conditions.

To assess the corrosion effects on the catalytic layer and PEM during the OCV test, we characterized the cross-sectional morphology of the MEAs before and after the test. The results are presented in Fig. 5. Before the endurance test, the PEM and cathode catalytic layer of the comparison MEA samples measured 15.6 µm and 5.6 µm in thickness, respectively. After 70 h of the OCV

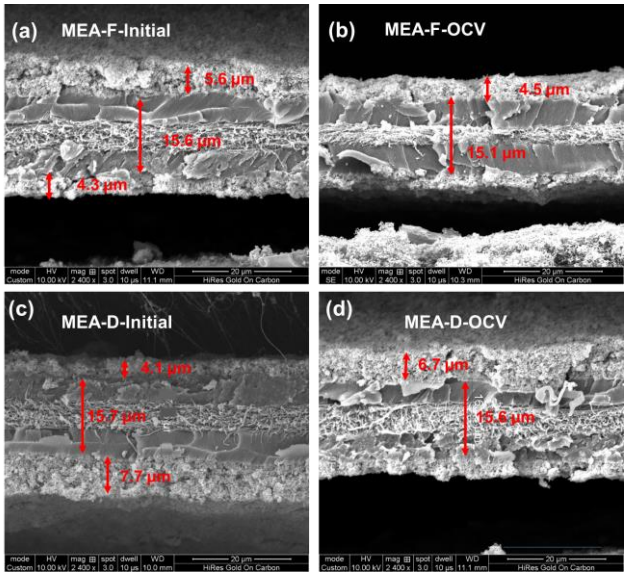

Fig. 5 Cross-sectional morphology of MEA-F sample (a) before and (b) after the open-circuit durability test, and MEA-D sample (c) before and (d) after the open-circuit durability test.

endurance test, these thicknesses decreased to 15.1 µm and 4.5 µm. Notably, the thickness of the PEM remained relatively stable, aligning with the hydrogen permeation current density over time. In contrast, the cathode catalytic layer experienced a significant reduction, decreasing by 1.1 µm, or 19.6%. This suggests that the free radicals generated during the OCV test, combined with the prolonged exposure to high cathode potentials (above 0.9 V), adversely affected the structure of the catalytic layer. This damage led to catalyst loss, a reduction in the thickness of the catalytic layer, and a decrease in the ECSA, ultimately impairing the power generation performance of the single cell. Fig. 5c and 5d illustrate the cross-sectional morphology of the MEA-D sample after the durability test. The thickness of the PEM remained nearly unchanged, indicating effective protection of the ionomer in this sample. However, the thickness of the cathode catalytic layer decreased from 7.7 µm to 6.7 µm, attributed to carbon corrosion resulting from the extended open-circuit state of the membrane electrodes. This finding underscores the importance of designing catalyst layers that can withstand both free radical generation and high

potential conditions to enhance durability and performance.

3.2 Cell reversal tolerance test

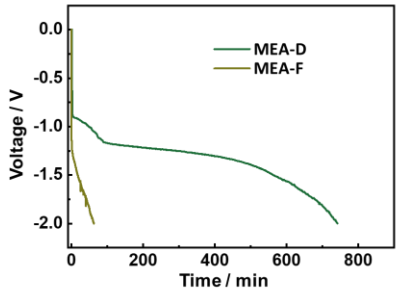

Fig. 6 Curve of cell voltage versus time during reversal testing of two membrane electrodes

To evaluate the anti-reversal performance of the membrane electrode, we conducted a series of tests where the initial performance of the single-cell was followed by a reversal assessment. The tests were carried out under controlled conditions—cell temperature was maintained at 80 °C, with relative humidity at 100%. The inlet pressures for the cathode and anode were set at 130 kPa and 120 kPa, respectively. A reversal current density of 200 mA cm^{-2} was applied, along with hydrogen and air flow rates of 0.3 mL min^{-1} each. During the test, single-cell voltage was monitored continuously, and testing was halted once the voltage dropped to -2.0 V. Fig. 6 illustrates the voltage-time curve recorded during the reversal test for the MEA-D. The results indicate that the unmodified membrane electrode exhibited an reversal performance time of only 60 minutes, while MEA-D demonstrated a significantly longer time of 742 minutes, reflecting an improvement of 92%. These findings suggest that MEA-D possesses excellent resistance to reversal conditions, highlighting its potential for enhanced durability in practical applications.

Fig. 7 presents a comparison of the power generation performance of the membrane electrode before and after the reversal test. The results demonstrate that MEA-D maintains excellent electrochemical performance post-test, with only minor degradation observed at current densities ranging from 200 to 1600 mA cm^{-2}. Notably, the maximum voltage drop at these current densities was just 24 mV. At a current density of 1000 mA cm^{-2}, MEA-D exhibited a voltage of 0.652 V, which is 24 mV lower than its pre-test value, corresponding to a decay rate of 2 mV h^{-1}. In contrast, the comparison sample showed a voltage drop of 51 mV at the same current density, with a significantly higher decay rate of 51 mV h^{-1}. This indicates that the incorporation of the anti-reversal catalyst in MEA-D effectively reduced the decay rate by 96%. Overall, these findings suggest that the reversal test has a minimal impact on the power generation performance of MEA-D, highlighting its robustness and durability.

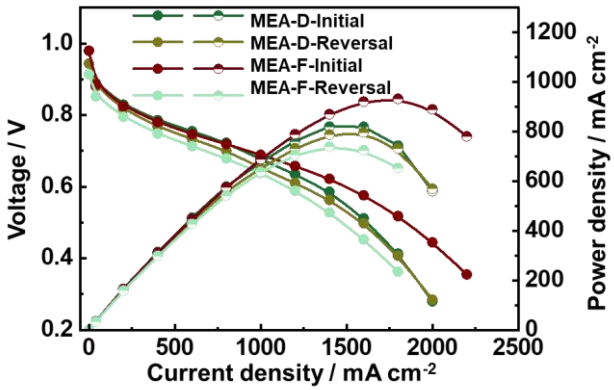

Fig. 7 Comparison of power generation performance before and after MEA-F and MEA-D reversal tests

4. CONCLUSIONS

In this chapter, we describe the fabrication of MEA-D, which was created by applying CZO as a radical quencher and $IrRuO_2$ as an anti-reversal catalyst to the cathode and anode sides of a single cell, respectively. We assessed the initial electrochemical performance of the single cell, focusing on its open-circuit durability and anti-reversal capabilities. Although MEA-D, which incorporated 10 wt. % CZO on the cathode and 20 wt. % RTA on the anode, exhibited slightly diminished power generation at high current densities compared to a single-cell MEA using commercial Pt/C catalysts, it demonstrated outstanding open-circuit durability. During a 500 h OCV test, voltage degradation was reversible. The hydrogen permeation current density varied between 5 and 8 mA cm^{-2}, showing no direct correlation with the inlet pressure difference across the anode and cathode. By the conclusion of the test, MEA-D maintained an open-circuit voltage of 0.945 V, with minimal change in the thickness of the PEM. Additionally, MEA-D displayed superior anti-reversal performance. The reversal time reached 742 minutes at a current density of 200 mA cm^{-2}, and the voltage at 1000 mA cm^{-2}, along with the maximum power density, only decreased by 24 mV and 23.2 mW cm^{-2}, respectively, following the first reversal test. These findings suggest that MEA-D offers a promising approach for developing durable membrane electrodes.

ACKNOWLEDGEMENT

The authors appreciate the Program of Ministry of Science & Technology of China (No. 2022YFB2502504) for financial support.

REFERENCE

[1] Staffell I, Scamman D, Velazquez Abad A, Balcombe P, Dodds PE, Ekins P, et al. The role of hydrogen and fuel cells in the global energy system. Energy & Environmental Science. 2019;12:463-91.

[2] Eberle U, Müller B, von Helmolt R. Fuel cell electric vehicles and hydrogen infrastructure: status 2012. Energy & Environmental Science. 2012;5.

[3] Ralph TR, Hudson S, Wilkinson DP. Electrocatalyst Stability In PEMFCs And The Role Of Fuel Starvation And Cell Reversal Tolerant Anodes. ECS Transactions. 2006;1:67-84.

[4] Taniguchi A, Akita T, Yasuda K, Miyazaki Y. Analysis of degradation in PEMFC caused by cell reversal during air starvation. International Journal of Hydrogen Energy. 2008;33:2323-9.

[5] Shao Y, Yin G, Gao Y. Understanding and approaches for the durability issues of Pt-based catalysts for PEM fuel cell. Journal of Power Sources. 2007;171:558-66.

[6] Sethuraman VA, Weidner JW, Haug AT, Motupally S, Protsailo LV. Hydrogen Peroxide Formation Rates in a PEMFC Anode and Cathode. Journal of The Electrochemical Society. 2008;155.

[7] Qiao J, Saito M, Hayamizu K, Okada T. Degradation of Perfluorinated Ionomer Membranes for PEM Fuel Cells during Processing with H[sub 2]O[sub 2]. Journal of The Electrochemical Society. 2006;153.

[8] Bi W, Gray GE, Fuller TF. PEM Fuel Cell Pt/C Dissolution and Deposition in Nafion Electrolyte. Electrochemical and Solid-State Letters. 2007;10.

[9] Kim L, Chung CG, Sung YW, Chung JS. Dissolution and migration of platinum after long-term operation of a polymer electrolyte fuel cell under various conditions. Journal of Power Sources. 2008;183:524-32.

[10] Zatoń M, Prélot B, Donzel N, Rozière J, Jones DJ. Migration of Ce and Mn Ions in PEMFC and Its Impact on PFSA Membrane Degradation. Journal of The Electrochemical Society. 2018;165:F3281-F9.

[11] Lim C, Alavijeh AS, Lauritzen M, Kolodziej J, Knights S, Kjeang E. Fuel Cell Durability Enhancement with Cerium Oxide under Combined Chemical and Mechanical Membrane Degradation. ECS Electrochemistry Letters. 2015;4:F29-F31.

[12] Endoh E. Development of Highly Durable PFSA Membrane and MEA for PEMFC Under High Temperature and Low Humidity Conditions. ECS Transactions. 2008;16:1229-40.

[13] Coms FD, Liu H, Owejan JE. Mitigation of Perfluorosulfonic Acid Membrane Chemical Degradation Using Cerium and Manganese Ions. ECS Transactions. 2008;16:1735-47.

[14] Gubler L, Koppenol WH. Kinetic Simulation of the Chemical Stabilization Mechanism in Fuel Cell Membranes Using Cerium and Manganese Redox Couples. Journal of The Electrochemical Society. 2011;159:B211-B8.

[15] Prabhakaran V, Arges CG, Ramani V. Investigation of polymer electrolyte membrane chemical degradation and degradation mitigation using in situ fluorescence spectroscopy. Proc Natl Acad Sci U S A. 2012;109:1029-34.

[16] Hong BK, Mandal P, Oh J-G, Litster S. On the impact of water activity on reversal tolerant fuel cell anode performance and durability. Journal of Power Sources. 2016;328:280-8.

[17] Mandal P, Hong BK, Oh J-G, Litster S. Understanding the voltage reversal behavior of automotive fuel cells. Journal of Power Sources. 2018;397:397-404.

[18] Ioroi T, Yasuda K. Highly reversal-tolerant anodes using Ti4O7-supported platinum with a very small amount of water-splitting catalyst. Journal of Power Sources. 2020;450.

[19] Wang Y, Xie X, Zhou C, Feng Q, Zhou Y, Yuan X-Z, et al. Study of relative humidity on durability of the reversal tolerant proton exchange membrane fuel cell anode using a segmented cell. Journal of Power Sources. 2020;449.

[20] You E, Lee SW, You D, Lee B, Pak C. Effect of Metal Composition and Carbon Support on the Durability of the Reversal-Tolerant Anode with IrRu Alloy Catalyst. Catalysts. 2020;10.

[21] Jang I, Hwang I, Tak Y. Attenuated degradation of a PEMFC cathode during fuel starvation by using carbon-supported IrO2. Electrochimica Acta. 2013;90:148-56.